

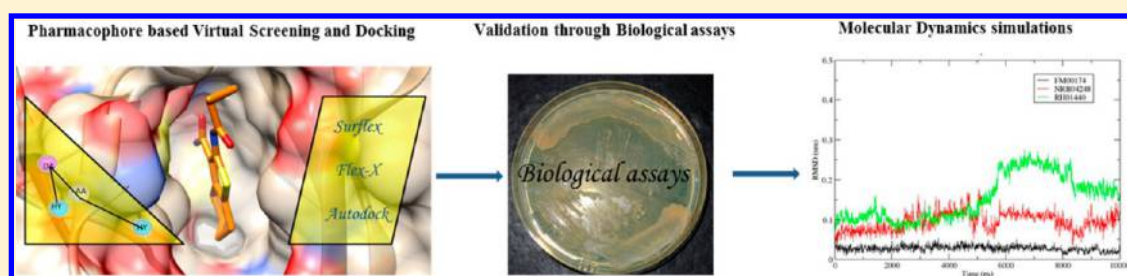
Identification of Novel Inhibitors of *Mycobacterium tuberculosis* PknG Using Pharmacophore Based Virtual Screening, Docking, Molecular Dynamics Simulation, and Their Biological Evaluation

Nidhi Singh,[†] Sameer Tiwari,[‡] Kishore K. Srivastava,^{‡,§} and Mohammad Imran Siddiqi^{*,†,§}

[†]Molecular and Structural Biology Division and [‡]Microbiology Division, CSIR–Central Drug Research Institute, Lucknow, UP 226031, India

[§]Academy of Scientific and Innovative Research, New Delhi 110025, India

Supporting Information



ABSTRACT: PknG is a Ser/thr protein kinase that plays a crucial role in regulatory processes within the mycobacterial cell and signaling cascade of the infected host cell. The essentiality of PknG in mycobacterial virulence by blocking phagosome–lysosome fusion as well as its role in intrinsic antibiotic resistance makes it an attractive drug target. However, only very few compounds have been reported as *Mycobacterium tuberculosis* PknG (MtPknG) inhibitors so far. Therefore, in an effort to find potential inhibitors against MtPknG, we report here a sequential pharmacophore-based virtual screening workflow, 3-fold docking with different search algorithms, and molecular dynamic simulations for better insight into the predicted binding mode of identified hits. After detailed analysis of the results, six ligands were selected for in vitro analysis. Three of these molecules showed significant inhibitory activity against MtPknG. In addition, inhibitory studies of mycobacterial growth in infected THP-1 macrophages demonstrated considerable growth inhibition of *M. bovis* BCG induced through compound NRB04248 without any cytotoxic effect against host macrophages. Our results suggest that the compound NRB04248 can be explored for further design and optimization of MtPknG inhibitors.

1. INTRODUCTION

Tuberculosis (TB) is a dreadful disease which has persisted in human beings since time immemorial as evident in primordial civilizations.^{1,2} It affects are seen around the globe with sub-Saharan Africa carrying the highest proportion of new cases per population while Asia accounts for 60% of new cases globally.³ The tuberculosis death rate has dropped significantly in the past due to an extensive implementation of DOTS and Stop TB strategy by the World Health Organization, but it has resurged as a public health threat with the advent of multi-drug-resistant TB (MDR-TB), extensively drug-resistant TB (XDR-TB),⁴ and totally drug-resistant TB (TDR-TB).⁵

Insight into *Mycobacterium*'s success tale depicts that its virulence is the result of its ability to survive within host macrophage for long time while normally internalized and phagocytised bacteria are degraded within phagolysosome. To dodge the defense surveillance system pathogens have evolved different approaches like escape from phagocytosis or to cope up the hostile environment of lysosome but pathogenic mycobacteria manage to prevent its fusion with lysosome therefore can survive for very long period of time.⁶ Apart from membrane

lipids and host proteins, mycobacterial protein kinases have been reported to be involved in escape mechanism of lysosome fusion.^{7,8} Eleven different serine/threonine kinases have been reported to be encoded by mycobacteria, and among them, PknG has been found to be essential for the survival in the host. It is intriguing to note the presence of PknG in the genome of *Mycobacterium leprae* that is considered to carry the minimal set of genes required for virulence, therefore, indicating the cardinal role of PknG in sustenance tactics inside the host macrophage.⁹ PknG has been found to be indispensable for in vitro growth of mycobacteria.^{10,11} In another subcellular localization studies it has been suggested that PknG is continuously secreted by pathogenic mycobacteria and is transferred into host cytosol offering an advantage as to block the PknG transport across lipid rich mycobacterial cell wall is not required.⁷ PknG has also been reported to be involved in acquiring intrinsic antibiotic resistance in mycobacteria.¹¹ All these findings suggest that PknG is a promising drug target.

Received: March 18, 2015

Published: May 12, 2015

Virtual screening is the computational analog of high throughput screening employed for the identification of inhibitors. It has proved its mettle in the present era of expanded chemical space and experimental structure availability in terms of cost and time efficacy. Several studies have been reported in literature which highlights the successful application of virtual screening in identification of novel inhibitors against various protein drug targets.^{12–16} It can be branched into ligand based, structure based, and combined approaches. In a ligand based approach, information from active ligands is harnessed and utilized to prioritize the library compounds usually through pharmacophore or QSAR based screening models,¹⁷ while a structure based mode requires that the three-dimensional structure of target protein and screening is performed usually through docking.¹⁸ Integration of machine learning models as filter or activity prediction models have added another dimension to virtual screening.¹⁹ Both ligand and structure based methods can be implemented in a stepwise fashion as in this work we have performed rational pharmacophore based virtual screening of the commercial small molecule Maybridge library using an earlier reported set of triazolylmethoxy aminopyrimidines as inhibitors of *MtPknG*. In the subsequent steps, docking with three well established docking programs with different search algorithms has been performed followed by visual inspection. After employing the above-mentioned approach, six molecules were selected for in vitro experiment and enzyme inhibition was determined by assessing kinase activity using ADP-Glo kinase assay kit and inhibition studies of mycobacterial growth in infected THP-1 macrophage cells was also done. To understand the binding mode and analyze the stability of proposed binding interactions, predicted binding complexes have been subjected to molecular dynamics simulations. *MtPknG* is a multidomain protein consisting of central kinase domain which is flanked by N-terminal rubredoxin and C-terminal tetratricopeptide repeat domain therefore exhibiting similar topology to eukaryotic kinases. The reported bound inhibitor AX20017 in the binding pocket of ATP showed the presence of unique set of amino acid residues that are not found in human kinases,²⁰ and therefore, the ATP binding site can be exploited for identifying inhibitors against *MtPknG*.

2. MATERIALS AND METHODS

2.1. Pharmacophore Hypothesis Generation and Virtual Screening. The set of triazolylmethoxy aminopyrimidines were reported to possess inhibitory activity against *MtPknG* by Anand et al.²¹ This data set was used for the pharmacophore hypothesis generation. The compounds were drawn by using the sketch module of the molecular modeling suite Sybyl 2.0.²² The geometries of these compounds were optimized using the Tripos force field and Gasteiger–Huckel charges.³⁰ The energy minimization was done using the Powell method with an energy convergence gradient of 0.001 kcal/mol. The top three inhibitors in terms of activity, namely compounds 9, 2, and 11 (Supporting Information, S1) were selected from this set of inhibitors against *MtPknG*, and a pharmacophore hypothesis was generated using the GASP²³ module of Sybyl-2.0. The genetic algorithm similarity program (GASP) is a genetic algorithm based program for the pharmacophore model generation through alignment of flexible molecules by superimposing them and fitting them to similarity constraints. Molecules are imitated as a chromosome in which conformational and intermolecular mapping information is ciphered. Conformational data comprises angles of rotation

about flexible bonds because it adjusts only torsion angles while searching for molecular alignment. Intermolecular feature mapping was done between hydrogen bond donor proton and acceptor lone pair and ring center feature. The molecular conformation that fits the constraints is allowed to produce more offspring similar to them. Alignment fitness is determined by number and similarity of features aligned, volume overlap of alignment and van der Waals energy of conformations. UNITY query was prepared by extracting pharmacophoric features and adding distance constraints to it. For the validation of the pharmacophore hypothesis, a test set database was prepared consisting of these 17 known inhibitors of *MtPknG* spiked into a subset of World of Molecular Bioactivity (WOMBAT) database consisting of 1207 molecules, active against different proteins other than used in the present study, considered here as inactive.²⁴ The flexible search methodology was employed as it takes into account the conformational flexibility of molecules. Virtual screening was carried out using these pharmacophore hypotheses for Maybridge small molecule database.²⁵

2.2. Comprehensive Molecular Docking and Scoring.

In order to reduce false positives the hits obtained from the pharmacophore based virtual screening were subjected to comprehensive docking using three well-established docking programs with different scoring algorithms namely Surflex-Dock,²⁶ Flex-X,²⁷ and AutoDock 4.2.²⁸ Surflex uses an empirical scoring function and a patented search engine to dock ligands into a protein's binding site and is based on the Hammerhead scoring function and a consensus score that is the linear combination of nonlinear functions of protein–ligand atomic surface distances.²⁶ The interactions include steric, polar, entropic, and solvation terms. In addition, a total score is also generated. Subsequently pharmacophore hits were also docked using Flex-X interfaced with sybyl7.1 and Autodock4.2. Flex-X employs a fast algorithm for flexible docking of small ligands into a fixed protein binding site using an incremental construction process in which the base fragment is selected automatically through pattern recognition technique of pose clustering and remaining portion of ligand is placed on the initial base incrementally. The score predicted is the estimate of free energy of binding of protein–ligand interactions.²⁷ Standard parameters of the Flex-X program as implemented in SYBYL7.1 were used during docking. AutoDock combines a rapid energy evaluation through pre calculated grids of affinity potential with a variety of search algorithms to find suitable binding positions for a ligand on a given protein.²⁸ The Lamarckian genetic algorithm, a modification of the traditional genetic algorithm, was used in this study. The hits having score above the cut off as predicted by all three docking algorithms were subjected to redocking with Surflex-geomx module to prioritize the compounds. The high scoring compounds were inspected visually, and the selected compounds were subjected to biological evaluation.

2.2.1. Receptor Preparation and Docking Validation. The crystal structure of PknG was retrieved from the protein databank (PDB: 2PZI), this is cocrystallized structure with bound inhibitor designated as AX20017.²⁰ Accuracy of the docking programs was checked by assessing their ability to reproduce the experimental conformation of AX20017 (bound inhibitor) in the active site of PknG. This substrate binding site was used to dock the hits obtained from screening. It utilizes the conserved ATP binding site and also show hydrophobic contacts with Ile-87 and Ala-92 of unique N-terminal segment. Other hydrophobic residues Ile-165, Val-179, Lys-181, Met-232, and

Ile-292 are present in the active site. Additionally, Val-235 and Glu-233 provide hydrogen bonding to the ligand. For receptor preparation in the Surflex program, ligand structure was extracted and isolated in separate file. The side chains of the protein structure then were fixed using default settings; water atoms were removed, hydrogen atoms were added, unknown atom types were assigned, and bumps were relaxed. The Kollman-all atom charges were assigned to protein atoms. Protomol was generated using the ligand based mode and docking was performed. The docking protocol was found to be fairly able to reproduce the experimental conformation. In the same manner, the bound conformation of AX20017 was reproduced using Flex-X and Autodock4.2. The docking was performed using standard parameters of the Flex-X program as implemented in Sybyl 7.1. Docking of ligands to MtPknG through Autodock4.2 was carried out using the Lamarckian genetic algorithm applying default parameters with an initial population of 150 randomly placed individuals and maximum number of generations set to 27 000. The grid maps were calculated with Autogrid4.2 and chosen to be centered at a ligand. The docked poses were analyzed, and RMSD with reference to the bound inhibitor AX20017 was calculated.

2.3. Biological Evaluation. **2.3.1. Purification of Mycobacterial PknG.** The compounds were screened against the mycobacterial serine threonine protein kinase G (PknG). The recombinantly purified enzyme was used for the study. *Mycobacterium tuberculosis* H37Rv (MTB) genomic DNA was used as a template for amplification of *PknG* gene by PCR. The gene was cloned in pTZ57R/T vector using the primers containing the *Hind*III restriction sites. For expression in *E. coli*, complete *PknG* ORF with *Hind*III was subcloned in pTriEx4 vector. *E. coli* BL21 (DE3) cells were transformed with pTriEX4-*PknG* plasmid, and transformants were grown in LB medium containing ampicillin (100 μ g/mL) at 37 °C, until OD₆₀₀ reached 0.6. IPTG was then added to a final concentration of 0.8 mM and cultures were further grown for overnight (16 h) at 22 °C with shaking at 180 rpm. Cells were harvested by centrifugation at 3500 rpm for 15 min and resuspended in [20 mM Tris-HCl (pH 7.4), 50 mM NaCl, 5 mM imidazole, 1 mM PMSF] and sonicated on ice for 20 min. After sonication, cell lysate was centrifuged at 13 000 rpm for 30 min and supernatant was loaded onto Ni²⁺-NTA column, prewashed with 50 mM imidazole and 6-His-PknG was eluted with 250 mM imidazole. Affinity purified 6-His-PknG was further purified by size exclusion chromatography using Sephacryl 200 column and AKTA Prime protein purification system (GE healthcare).

2.3.2. Screening of Compounds by ADP-Glo Kinase Assay. The compounds were dissolved completely in DMSO. For the determination of primary efficacy, 100 μ M concentration of each compound was screened using purified PknG as an enzyme. The activity and the inhibition were determined by using luciferase activity mediated by ATP, by ADP-Glo kinase assay kit (Promega, USA). Briefly, ADP-Glo is a luminescent kinase assay that measures ADP formed from a kinase reaction. ADP is converted into ATP, which is converted into light by Ultra-Glo Luciferase. The active PknG enzyme was incubated with different concentrations of compounds containing 1X kinase buffer (40 mM Tris, 20 mM MgCl₂, 2 mM MnCl₂, 2 mM DTT, 0.1 μ g/mL BSA) for 1 h at 24 °C. ADP-Glo reagent was then added to the reaction, and the incubation was continued for 45 min. The kinase detection reagent (KDR) was subsequently added to the reaction and incubated for 30 min at

24 °C. The inhibition of auto phosphorylation of kinase by the compounds was measured by luminometer (Berthold).

2.3.3. THP-1 Macrophage Infection with *M. bovis* BCG. The human monocytic cell line THP-1 was purchased from ATCC, USA. THP-1 cells were cultured in RPMI 1640 (Sigma-Aldrich) supplemented with 10% FCS (CellClone, Life Technologies) and incubated at 37 °C plus 5% CO₂. For infection experiments, 3 \times 10⁵ THP-1 cells/mL were passaged in complete RPMI containing 30 ng/mL phorbol myristate acetate (PMA, Sigma-Aldrich) and plated for differentiation to macrophages. After 48 h, supernatants were removed and log phase *M. bovis* BCG culture used to infect THP-1 cells at multiplicity of infection (MOI) of 10:1 (10 bacteria/1 cell) for 3 h. Cells were then washed four times with complete RPMI to remove extracellular bacilli. Compounds were added at various concentrations with fresh RPMI medium and incubated for 24 h. After 48 h, the infected cells were lysed for 5 min at room temperature in distilled water containing 0.05% SDS to determine the numbers of CFU/mL on Middlebrook 7H10 agar. The experiments were carried out in triplicate.

2.3.4. Cytotoxicity Assay by MABA Assay. The cytotoxicity assays was performed as previously reported^{29,30} with slight modification. Macrophages were harvested from subconfluent monolayers. The suspended cells were seeded in 96-well microplates, at an approximate initial density of 1 \times 10⁶ per well, in RPMI-1640 medium. Compounds were added at the concentrations from 100 μ M to 12.5 μ M. Rifampicin was taken as positive control for showing viability at concentrations from 4 to 0.5 μ g/mL. Also, 96-well plates were incubated for 48 h at 5% CO₂ at 37 °C. After 48 h, the resazurin was added and incubated for 4 h. The fluorescence and absorbance were measured in a spectrophotometer at 535/590 nm. Cytotoxicity was determined by comparing the resulting fluorescence with the mean fluorescence of the control wells (untreated cells) and was expressed as a percentage of cell viability. The 50% cytotoxic concentration (CC₅₀) is defined as the quantity of compound generating 50% of cell viability, compared to the control. The values of the percentages of cell viability were plotted against the concentrations, and CC₅₀ was determined. Experiments were carried out in triplicate.

2.4. Molecular Dynamics Simulations. To investigate the stability of predicted binding mode of identified hits, the complexes were subjected to molecular dynamics simulations using GROMACS 4.6.5 package.³¹ Systems were solvated in a cubic box with TIP3P water molecules at 12 Å marginal radiuses. At physiological pH, the structure was found to have negative charge, thus to make the system electrically neutral, 14 sodium ions were added in the simulation box using a "genion" tool. The solvent molecules were relaxed while all solute atoms were harmonically restrained to their original positions with force constant for 5000 steps. Emtol convergence criterion was set to 10.0 kJ/mol. Then, whole molecular systems were subjected to energy minimization by steepest descent minimization algorithm. Isotropic pressure coupling was performed using Parrinello–Rahman method. Electrostatic interactions were computed using the particle mesh Ewald method. Van der Waals and Coulomb interactions were truncated at 1.0 nm. Conformations were stored every 8 ps. Finally, systems were subjected to molecular dynamics (MD) simulation for 10 ns.

3. RESULTS AND DISCUSSION

3.1. Pharmacophore Model Generation and Virtual Screening. A set of aminopyrimidines were reported to

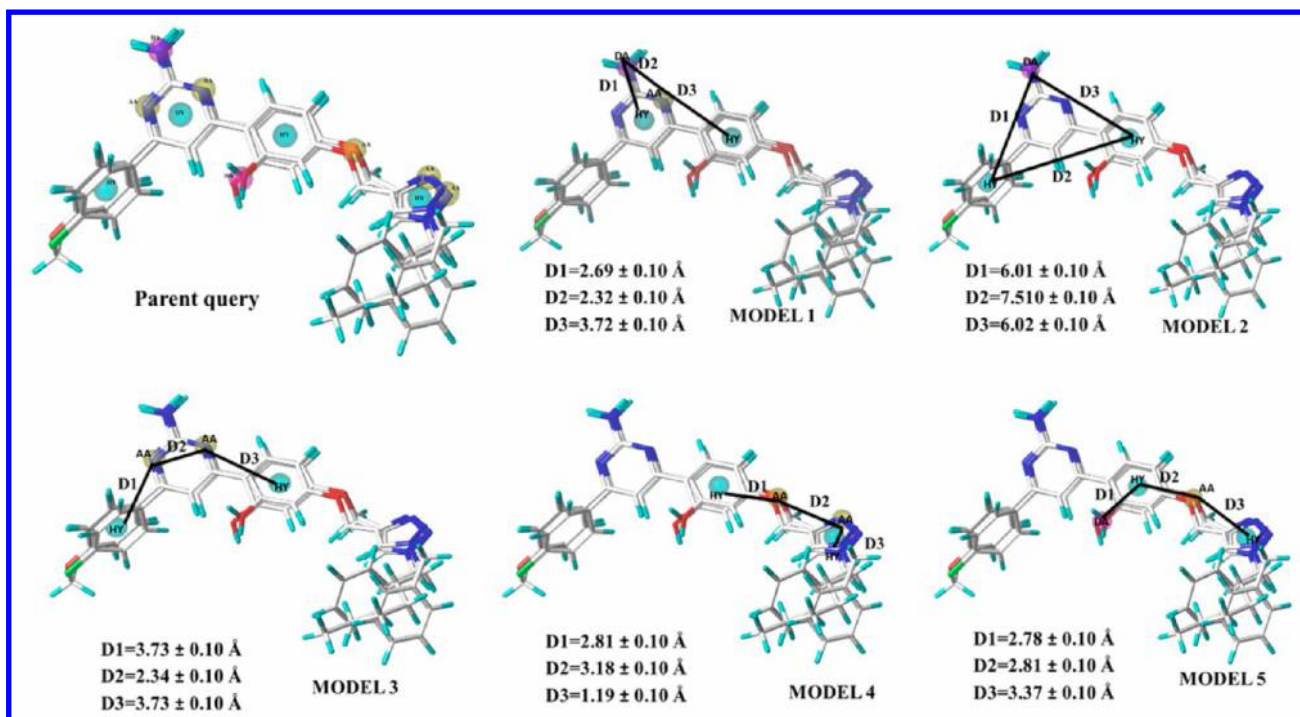


Figure 1. Parent query and pharmacophore models. The hydrophobic feature is shown in cyan, acceptor atom feature, in yellow, and donor atom feature, in purple. D1, D2, and D3 are the distances among these features. Sphere sizes indicate query tolerances.

Table 1. Statistical Parameters from Screening *MtPknG* Test Set Molecules

parameter	model 1	model 2	model 3	model 4	model 5
total no. of molecules in database (<i>D</i>)	1224	1224	1224	1224	1224
total no. of actives (<i>A</i>)	17	17	17	17	17
total hits (<i>H_t</i>)	16	62	38	143	40
active hits (<i>H_a</i>)	11	11	11	10	6
% yield of actives ($H_a/H_t \times 100$)	68.7	17.74	28.9	6.99	15.0
% ratio of actives ($H_a/A \times 100$)	64.70	64.70	64.70	58.8	35.2
enrichment factor (EF) ^a	49.5	12.77	20.84	5.03	10.8
false positives (<i>H_t</i> - <i>H_a</i>)	5	51	27	133	34
false negatives (<i>A</i> - <i>H_a</i>)	6	6	6	7	11
goodness of hit score (GH) ^b	0.6745	0.2823	0.3703	0.1775	0.1950

^aEF = $H_a D / H_t A$. ^bGH = $(H_a / 4 H_t A) (3A + H_t) \{1 - [(H_t - H_a) / (D - A)]\}$.

possess inhibitory activity against *MtPknG* by Anand et al.²¹ The crystal structure of *MtPknG* is available in complex with bound ligand AX20017. In order to integrate the ligand and structure based information we have derived pharmacophore model using set of aminopyrimidines and assessed it in relation to bound ligand AX20017. The top three compounds from aminopyrimidines series in terms of activity were used for pharmacophore alignment using the GASP program. The resultant pharmacophore hypothesis consisted of 11 pharmacophoric features, including 4 hydrophobic, 5 acceptor, and 2 donor atom features as seen in Figure 1 (parent query). The UNITY query including all 11 features of parent query did not yield significant hits. For rational selection of desired pharmacophoric features, different models were generated based on the pharmacophoric features from the parent query and their statistical evaluation was done.

3.1.1. Statistical Validation. A test set database was prepared consisting of these 17 known inhibitors of *MtPknG* spiked into a subset of the World of Molecular Bioactivity (WOMBAT) database consisting of 1207 molecules, active against different

proteins other than used in present study, considered here as inactive. The ability of pharmacophore to retrieve maximum number of active hits and rejection of inactive ones reflects its efficacy. Therefore, various statistical parameters were calculated such as enrichment factor (EF), goodness of hit (GH), % ratio of actives, % yield of actives, false positives, and false negatives. The various parameters for all the models are summarized in Table 1, and the models are shown in Figure 1. Among them, pharmacophore model 1 had an enrichment factor of 49.5, goodness of hit score of 0.6745, percentage ratio of actives of 64.70, and percentage yield of actives of 68.7 and is statistically significant.

3.1.2. Structural Analysis of Binding Pocket and Assessment of Selected Pharmacophore. To further assess the suitability of model 1 for virtual screening and possible contribution of pharmacophoric features in protein–ligand interaction, a detailed structural analysis was done. The reported inhibitor AX20017 occupies the ATP binding pocket which largely comprises the hydrophobic residues. The NH₂ group attached to the tetrahydrobenzothiophene ring acts as a

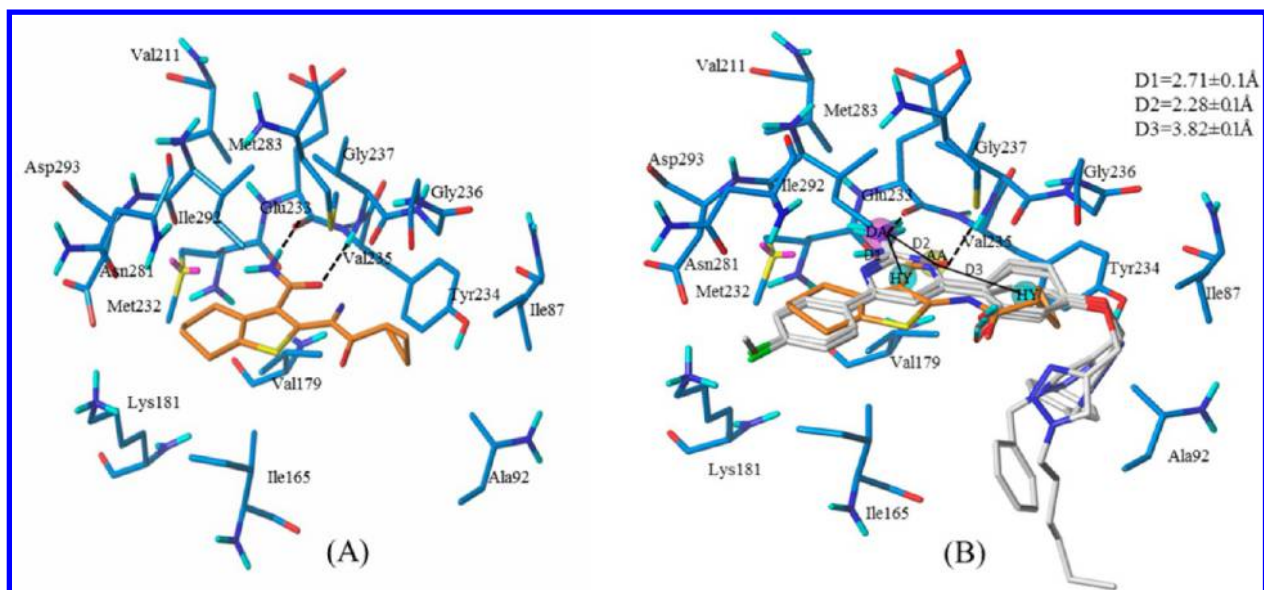


Figure 2. (A) Interaction pattern of bound ligand AX20017 in active site of *MtPknG* (PDB: 2PZI). (B) Bound inhibitor AX20017 and docked conformation of three compounds used in pharmacophore modeling aligned for common pharmacophore features shown in the active site of *MtPknG*. AX20017 is shown as orange in color. The other ligands are shown as atomtype, and active site residues are shown blue in color.

hydrogen donor and forms a hydrogen bond with Glu-233:O, and Val-235:NH forms another hydrogen bond with the amido substituent of the thiophene ring of the inhibitor. This hydrogen bonding places rest of inhibitor well to utilize the hydrophobic contacts (Figure 2A). To probe the binding mode of reported active compounds used in pharmacophore model generation, we docked them into the AX20017 binding site. The docked poses of top three active compounds which were earlier used in pharmacophore generation and bound inhibitor AX20017 were aligned for common pharmacophoric features. The aligned pharmacophoric features were found to map closely to the pharmacophoric features as proposed in model 1, consisting of two hydrophobic, one donor atom, and one acceptor atom features. Three out of four features overlapped, viz., donor atom, acceptor atom, and hydrophobic feature while the other hydrophobic feature connected to donor atom was present in both but not overlapped (Figure 2B). The donor atom feature is mapped to hydrogen bonding with Glu233, and the acceptor atom feature is positioned to facilitate hydrogen bonding with Val-235 which is reminiscent of one made to adenosine moiety of ATP; meanwhile, one hydrophobic feature packs against side chains of Ile-87, Ala-92, Ile-157, Gly-236, and Met283 and the other hydrophobic feature corresponds to contacts with side chains of Ile-165, Val-179, Met-232, and Ile-292. Together based on statistical evaluation and structural analysis model 1 was selected, and virtual screening was carried out.

3.1.3. Virtual Screening. The pharmacophore model 1, with minimal false positives and negatives, good enrichment factor and goodness of fit score, and taking in account the interaction profile as mentioned above, was considered as the best model for virtual screening among the different combinations of features of pharmacophore hypothesis and was selected for the further screening of the Maybridge small molecule database consisting of 54 275 molecules. Virtual screening was carried out using the flex utility of UNITY module available with SYBYL 2.0.²² Pharmacophore based virtual screening yielded 826 hits that met the specified requirements.

3.2. Docking and Scoring. The hits obtained from the pharmacophore based screening were docked into substrate binding cavity using Surflex, Flex-X, and Autodock4.2. We optimized the docking parameters of all the three docking programs by reproducing the binding pose of bound inhibitor AX20017 in all the three docking programs and the compounds from virtual screening hits were docked into the same binding site. The calculated root-mean-square deviation for the docked poses compared to crystal structure bound conformation was found to be 0.15, 0.30, and 0.73 Å for Surflex, Flex-X, and Autodock4.2, respectively (Figure 3).

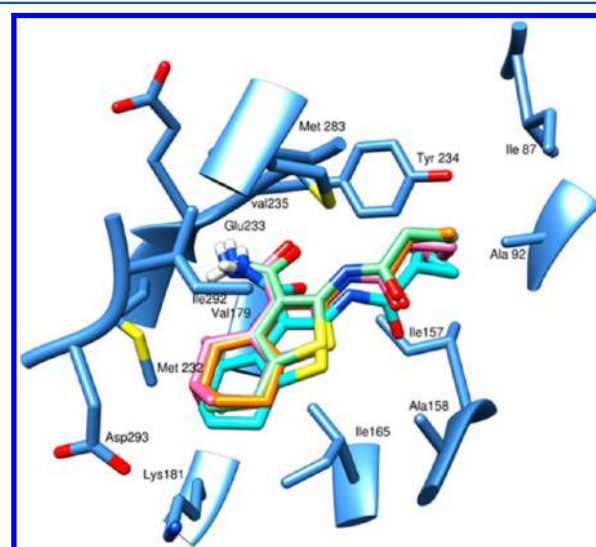
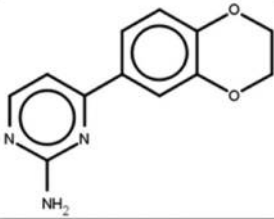
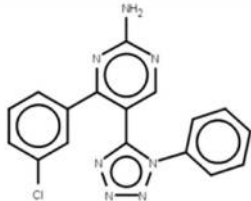
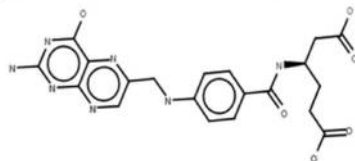
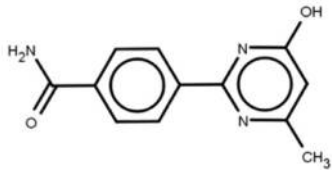
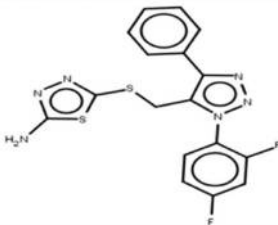
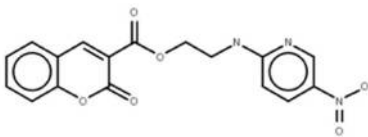


Figure 3. Reproduced docked conformations of AX20017 by using Surflex (green), Flex-X (pink), and Autodock4.2 (cyan) superimposed on bound crystal structure conformation (orange).

In order to reduce the number of false positives, the hits possessing docking score above set cutoff score in all three docking programs were selected. For Surflex it was set to total score as 3.82 which represents binding affinity in $-\log_{10}(K_d)$

Table 2. Selected Hits for Biological Assays

S.no	Name	Structure	Surflex score	Flex-X score	Autodock score
1.	FM00174		5.670	-22.130	-8.05
2.	NRB04248		5.720	-19.970	-9.50
3.	RH01440		7.180	-26.780	-8.53
4.	RJF00785		6.120	-22.060	-8.15
5.	CD08690		6.530	-23.420	-9.85
6.	BTB05500		7.110	-24.35	-9.27

units, for Flex-X docking energy of -17.0 kJ/mol and binding energy of -8.0 kcal/mol for Autodock. The cutoff was based on docking score of bound inhibitor taken as reference in respective docking programs. A total of 177 hits were obtained after employing docking score filter. These hits were redocked using surflex-geomx mode and were ranked according to the total score. The surflex-geomx mode was run for accuracy and differs from screening mode with regard to spin density of alignment method, for screen mode it is 3 while for geomx mode it is 9; therefore, dense search is performed in geomx mode, and accuracy is enhanced. In pursuit of selection of promising hits, visual inspection of compound binding mode was done and the following criteria were considered: (1) protein ligand surface complementarity, (2) formation of hydrogen bond with Val235 and Glu233 or any other residue, (3) hydrophobic contacts. Taking in account the docking score and visual

inspection, six compounds were finally purchased and subjected to the biological evaluation. These six compounds possess the pharmacophoric features, namely, one donor atom feature, one acceptor atom feature, and two hydrophobic features, and maps well to the selected pharmacophore model 1 which is constructed from the subset of three most active compounds out of set of 17 aminopyrimidines compounds reported earlier possessing inhibitory activity against *MtPknG*. Structures and docking scores of the hits selected for biological evaluation are listed in Table 2.

3.3. Bio Evaluation of Compounds against Mycobacterial PknG. **3.3.1. Inhibition of Kinase Activity by ADP-Glo Kinase Assay.** The compounds proposed for in vitro analysis were screened as inhibitors of kinase activity of PknG by determining the autophosphorylation of the enzyme. The activity was determined by quantification of the ADP generated

by the kinase using the ADP-Glo assay kit (Promega, USA). The compounds BTB 05500, CD 08690, FM 00174, RH 01440, RJF 00785, and NRB 04248 showed 24, 15, 78, 33, 17 and 43% inhibition respectively against *MtPknG* at 25 μ M (Figure 4).

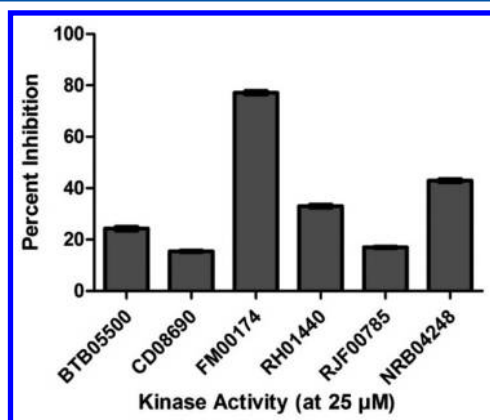


Figure 4. Kinase activity of different compounds by ADP-Glo kinase assay: percent inhibition shown at 25 μ M. The experiment was done in triplicate, and standard error mean (SEM) was calculated.

3.3.2. Inhibition of Mycobacterial Growth in Infected THP-1 Macrophage Cells. In order to see the effect of compounds on intracellular mycobacteria we have treated infected THP-1 cells and found that NRB04248 treatment has decreased CFU count as compared to untreated (Figure 5). The compound NRB 04248 was able to inhibit the growth of *M. bovis* BCG with 21% and was found to be nontoxic below 400 μ M. Other

compounds were shown to be toxic at 200 μ M by the cytotoxicity assay (Figure 5C). Recombinant BCG-Lux was treated with compound at different concentrations and in vitro mycobacterial growth in Sauton's medium was evaluated using the luciferase assay.³² The data showed lesser effect of compounds on mycobacterial growth as compared to Rifampicin (Figure 5B).

3.4. Proposed Mode of Binding of Active Compounds.

3.4.1. Molecular Docking. Docking predicted binding modes for the top three compounds (FM00174, NRB04248, and RH01440) showing significant inhibition in the kinase assay are shown in Figure 6. All of these compounds are predicted to bind in the pocket in a fashion similar to AX20017 as evident by the hydrogen bond formation pattern. All the three compounds show hydrogen bond formation with residues Glu-233 and Val-235 corresponding to donor atom and acceptor atom feature of pharmacophore while RH01440 can possibly form additional hydrogen bond with Lys181. The hydrophobic contacts are driven by residues Ile-157, Val179, Ala-158, Ile-165, Met-232, Ile-292, Ile-87, and Ala-92. The docked binding pose of FM00174 is shown in Figure 6A. The amine group attached to pyrimidine ring acts as hydrogen donor and forms hydrogen bond with residue Glu-233, the nitrogen of pyrimidine ring acts as hydrogen acceptor and forms the hydrogen bond with residue Val-235 while the hydrophobic contacts are driven by Ala-158, Ile-165, Met-283, Val-179, and Ile-292. The docked binding pose of NRB04248 (Figure 6B) speculates the formation of hydrogen bond with residue Glu-233 where amine group is acting as hydrogen donor and hydrogen bond with Val-235 is facilitated by nitrogen of pyrimidine ring acting as acceptor and is stabilized by well-placed hydrophobic

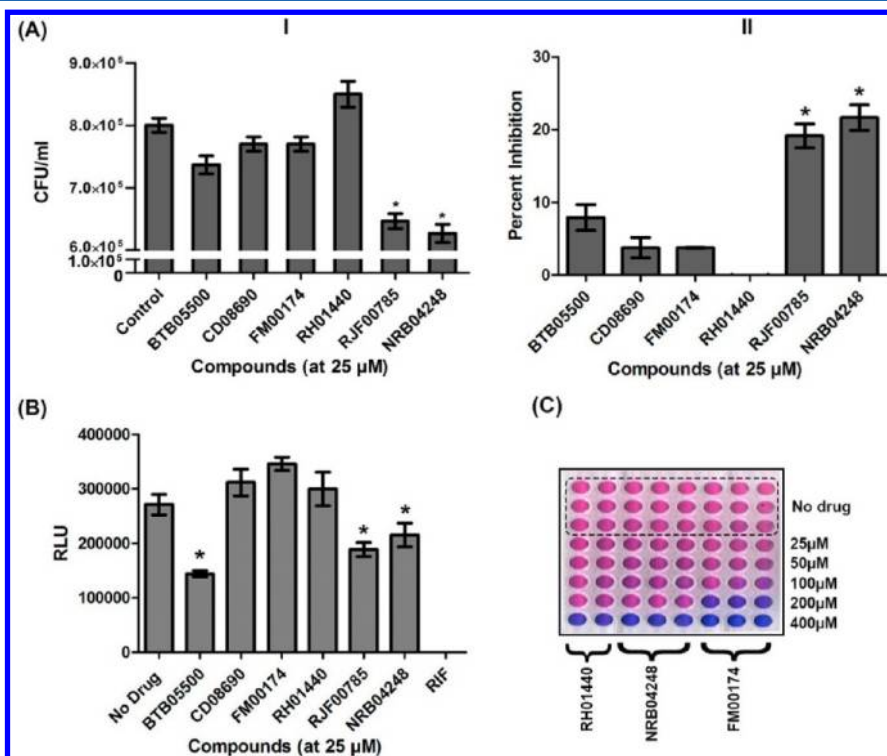


Figure 5. Survival of mycobacteria in THP-1 macrophage cells. (A) The infected macrophages were treated with 25 μ M of compounds (I). Treated and untreated *M. bovis* BCG were scored for the CFU/mL after one month of plating, and the percent inhibition was calculated as compared to control (II). (B) Mycobacterial growth was measured by luciferase assay (p value < 0.05). Rifampicin (RIF) was taken as a control (C) CC₅₀ of the compounds was determined by cytotoxicity assay (MABA assay).

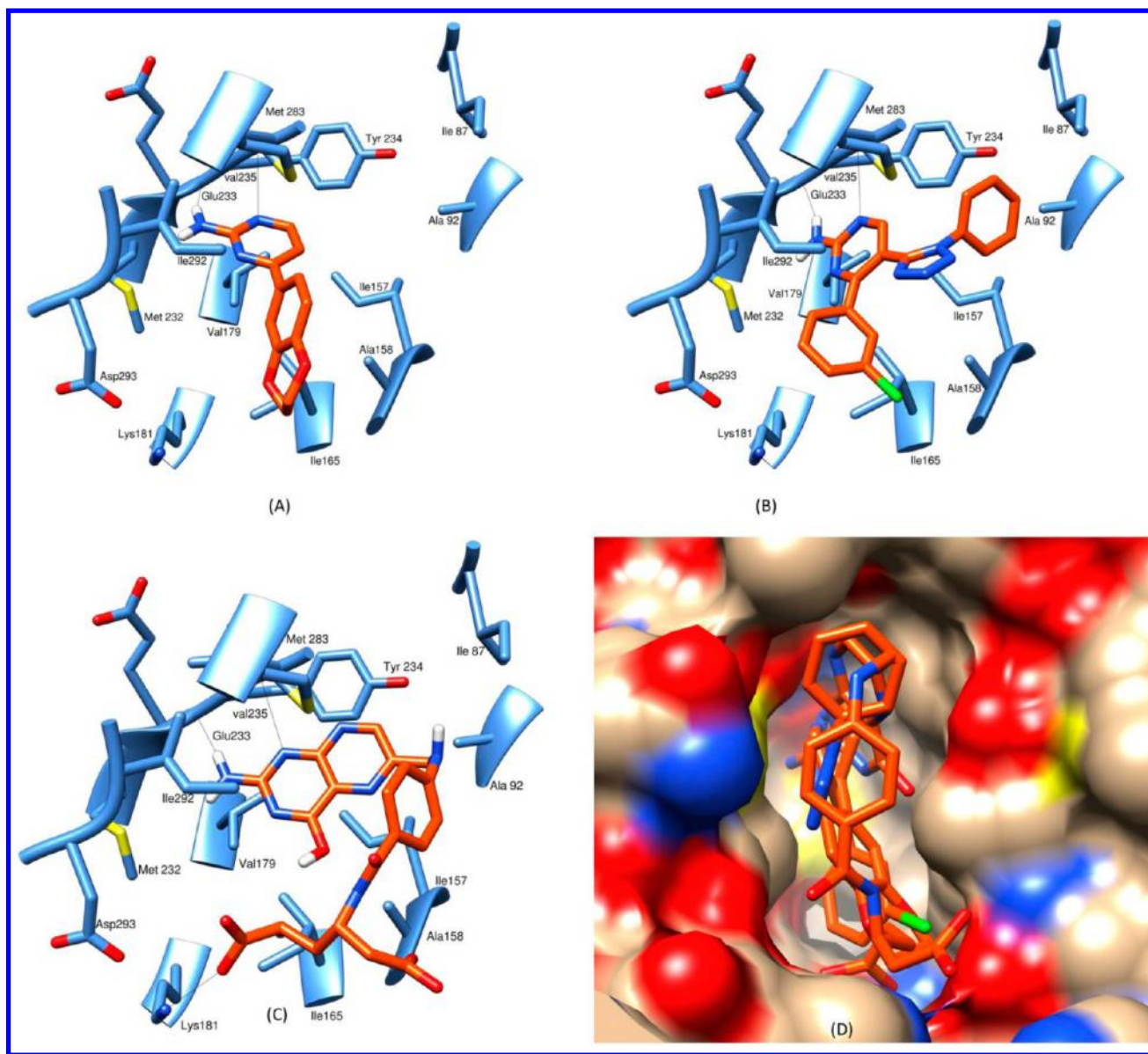


Figure 6. Docked pose of active compounds in the PknG binding site: (A) FM00174, (B) NRB04248, and (C) RH01440. (D) Surface view of protein active site and docked ligand poses. Hydrogen bonds are shown as black lines, protein residues are blue in color, and compounds are orange in color.

contacts since it contains three π -ring systems which provides extensive π -alkyl and π -sigma interactions. The pyrimidine and chlorophenyl ring is packed against Ile-165, Met-232, Ile-292, Val-179, and Ala-158 while the phenyl ring adjacent toazole ring is in contact with side chain of residues Ile-87, Ala-92, Tyr-234, and Ile-157. The interaction profile of RH01440 projects the formation of hydrogen bonds between hydroxy-pteridine ring system and Glu-233 and Val-235; the possibility of other hydrogen bonds exists through hexanedioic acid part of ligand with Lys-181 while the hydrophobic contacts are retained as mentioned above (Figure 6C).

3.4.2. Molecular Dynamics Simulation. For a stronger hypothesis and a better insight into the validity of the docking results achieved as well as to probe the overall binding mode stability of compounds we have conducted 10 ns long molecular dynamics simulations for the formerly mentioned protein–ligand complexes, viz., FM00174, NRB04248, and RH01440. The ligand RMSD was calculated and plotted for all of the

systems starting from the end of the equilibration phase and the interaction patterns were inspected for the maintenance of docking predicted hydrogen bonds as well as hydrophobic contacts for postproduction of molecular dynamics. The RMSDs of ligands were analyzed and were found to be lowest and most stable for FM00174; meanwhile for NRB04248, the RMSD fluctuated around 0.1 nm and was found stable. For RH01440, it deviated up to 0.25 nm between 5 and 7 ns and became stable onward therefore indicating the stability of docking predicted binding poses (Figure 7A). The average RMSDs of the protein backbone atoms were found to be 0.21, 0.25, and 0.26 nm for protein–ligand complexes of FM00174, NRB04248, and RH01440, respectively (Figure 7B). The root-mean-square fluctuation (RMSF) analyses highlighted possible protein movements involving residues Val-235 and Glu-233 for the predicted complexes (Figure 7C). The MD trajectories were analyzed for the presence and occupancy of proposed hydrogen bonds. The hydrogen bonds predicted between the

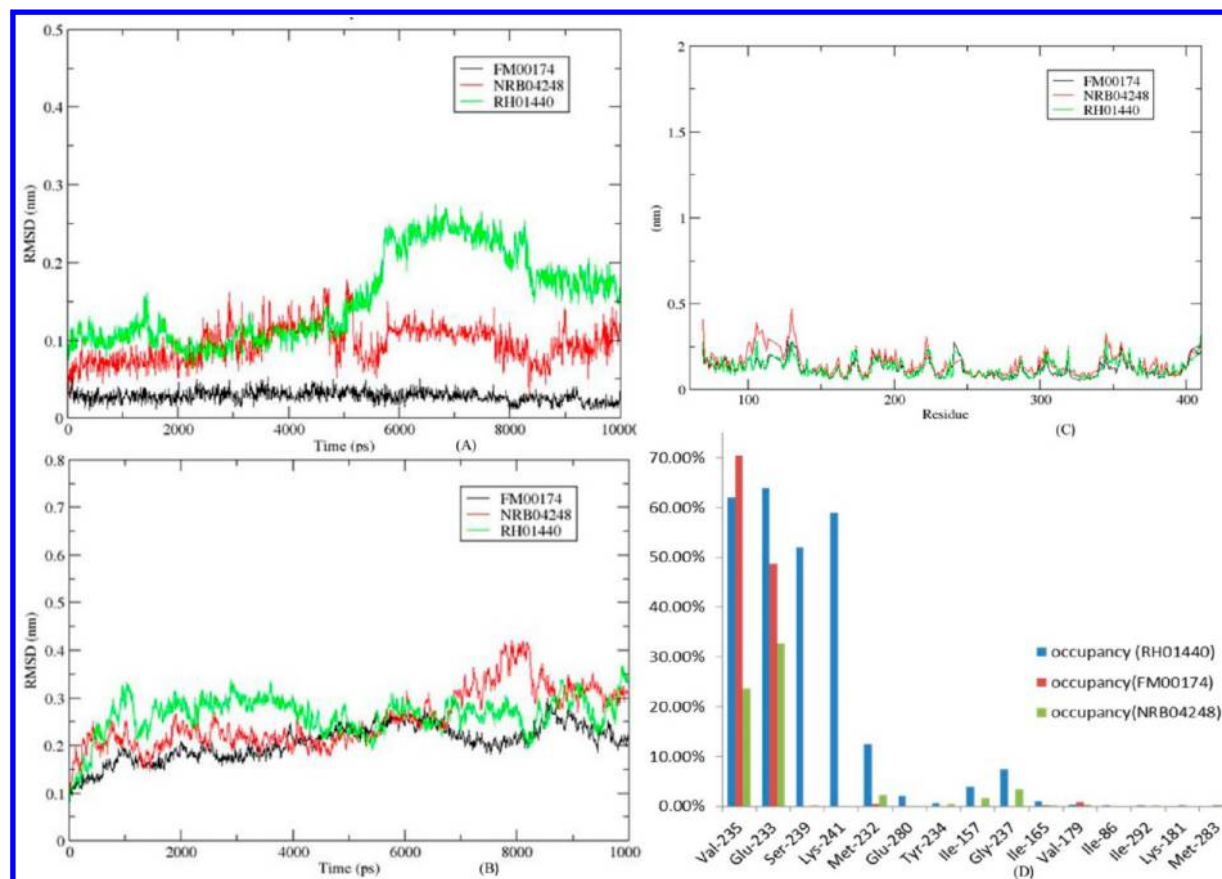


Figure 7. (A) RMSDs of ligands during 10 ns long simulation. (B) RMSDs of the protein in complex with docked ligands backbone atoms. (C) RMSFs during molecular dynamics trajectories for the docking predicted protein–ligand complexes. The graph is shown in black for FM00174, red for NRB04248, and green for RH01440. (D) Occupancy of proposed hydrogen bonds during MD trajectory for FM00174, NRB04248, and RH01440.

ligand and residues Val-235 and Glu-233 were found to be maintained for the major part of trajectory with high occupancy for all the three proposed compounds (Figure 7D). For RH01440 two additional hydrogen bonds with residues Lys-241 and Ser-239 were also found to have significant occupancy.

4. CONCLUSION

The implications of PknG in the pathogenesis and survival of the tubercle bacillus within a host by blocking phagosome–lysosome fusion and its role in intrinsic antibiotic resistance makes it an attractive drug target. Only a few inhibitors of *MtPknG* are reported yet; therefore in pursuit of finding potential inhibitors against *MtPknG*, we have performed pharmacophore based screening integrated with comprehensive three-fold docking. Molecular dynamics simulations were done to probe the binding mode and stability of predicted protein–ligand complexes. The applied virtual screening workflow led to the identification of novel inhibitors of *MtPknG*. Six compounds were subjected to kinase assay, and three of these molecules possessed significant inhibitory activity. In addition survival studies of mycobacterial growth in infected THP-1 macrophage cells resulted in the identification of compound NRB04248 which was able to inhibit the growth of *M. bovis* BCG and found to be nontoxic against the host macrophages. The above findings suggest that NRB04248 can be explored for the further development of new and more potent inhibitors of *MtPknG*.

■ ASSOCIATED CONTENT

Supporting Information

Structure of compounds used for pharmacophore generation. The Supporting Information is available free of charge on the ACS Publications website at DOI: 10.1021/acs.jcim.5b00150.

■ AUTHOR INFORMATION

Corresponding Author

*E-mail: mi_siddiqi@cdri.res.in, imsididi@yahoo.com.

Notes

The authors declare no competing financial interest.

■ ACKNOWLEDGMENTS

Work reported in this project is supported by a grant from CSIR network project GENESIS (BSC0121). N.S. acknowledges CSIR for a fellowship. CSIR-CDRI communication number allotted to this manuscript is 8991.

■ REFERENCES

- (1) Azizi, M. H.; Bahadori, M. A brief history of tuberculosis in Iran during the 19th and 20th centuries. *Arch Iran Med.* **2011**, *14* (3), 215–219.
- (2) Ziskind, B.; Halioua, B. Tuberculosis in ancient Egypt. *Rev. Mal Respir.* **2007**, *24* (10), 1277–1283.
- (3) <http://www.who.int/mediacentre/factsheets/fs104/en/index.html> (accessed Feb 15, 2013).

- (4) Jain, A.; Mondal, R. Extensively drug-resistant tuberculosis: current challenges and threats. *FEMS Immunol Med. Microbiol.* **2008**, *53* (2), 145–150.
- (5) Velayati, A. A.; Farnia, P.; Masjedi, M. R.; Ibrahim, T. A.; Tabarsi, P.; Haroun, R. Z.; Kuan, H. O.; Ghanavi, J.; Farnia, P.; Varahram, M. Totally drug-resistant tuberculosis strains: evidence of adaptation at the cellular level. *Eur. Respir. J.* **2009**, *34* (5), 1202–1203.
- (6) Nguyen, L.; Pieters, J. The Trojan horse: survival tactics of pathogenic mycobacteria in macrophages. *Trends Cell Biol.* **2005**, *15* (5), 269–276.
- (7) Walburger, A.; Koul, A.; Ferrari, G.; Nguyen, L.; Prescianotto-Baschong, C.; Huygen, K.; Klebl, B.; Thompson, C.; Bacher, G.; Pieters, J. Protein kinase G from pathogenic mycobacteria promotes survival within macrophages. *Science* **2004**, *304* (5678), 1800–1804.
- (8) Nguyen, L.; Walburger, A.; Houben, E.; Koul, A.; Muller, S.; Morbitzer, M.; Klebl, B.; Ferrari, G.; Pieters, J. Role of protein kinase G in growth and glutamine metabolism of *Mycobacterium bovis* BCG. *J. Bacteriol.* **2005**, *187* (16), 5852–5856.
- (9) Cole, S. T.; Eiglmeier, K.; Parkhill, J.; James, K. D.; Thomson, N. R.; Wheeler, P. R.; Honoré, N.; Garnier, T.; Churcher, C.; Harris, D.; Mungall, K.; Basham, D.; Brown, D.; Chillingworth, T.; Connor, R.; Davies, R. M.; Devlin, K.; Duthoy, S.; Feltwell, T.; Fraser, A.; Hamlin, N.; Holroyd, S.; Hornsby, T.; Jagels, K.; Lacroix, C.; Maclean, J.; Moule, S.; Murphy, L.; Oliver, K.; Quail, M. A.; Rajandream, M. A.; Rutherford, K. M.; Rutter, S.; Seeger, K.; Simon, S.; Simmonds, M.; Skelton, J.; Squares, R.; Squares, S.; Stevens, K.; Taylor, K.; Whitehead, S.; Woodward, J. R.; Barrell, B. G. Massive gene decay in the leprosy bacillus. *Nature* **2001**, *409* (6823), 1007–1011.
- (10) Av-Gay, Y.; Everett, M. The eukaryotic-like Ser/Thr protein kinases of *Mycobacterium tuberculosis*. *Trends Microbiol.* **2000**, *8* (5), 238–244.
- (11) Wolff, K. A.; Nguyen, H. T.; Cartabuke, R. H.; Singh, A.; Ogwang, S.; Nguyen, L. Protein kinase G is required for intrinsic antibiotic resistance in mycobacteria. *Antimicrob. Agents Chemother.* **2009**, *53* (8), 3515–3519.
- (12) Chan, F. Y.; Sun, N.; Neves, M. A.; Lam, P. C.; Chung, W. H.; Wong, L. K.; Chow, H. Y.; Ma, D. L.; Chan, P. H.; Leung, Y. C.; Chan, T. H.; Abagyan, R.; Wong, K. Y. Identification of a new class of FtsZ inhibitors by structure-based design and *in vitro* screening. *J. Chem. Inf. Model.* **2013**, *53* (8), 2131–2140.
- (13) Pauli, I.; dos Santos, R. N.; Rostirolla, D. C.; Martinelli, L. K.; Ducati, R. G.; Timmers, L. F.; Basso, L. A.; Santos, D. S.; Guido, R. V.; Andricopulo, A. D.; Norberto de Souza, O. Discovery of new inhibitors of *Mycobacterium tuberculosis* InhA enzyme using virtual screening and a 3D-pharmacophore-based approach. *J. Chem. Inf. Model.* **2013**, *53* (9), 2390–401.
- (14) Elhefnawi, M.; ElGamacy, M.; Fares, M. Multiple virtual screening approaches for finding new hepatitis C virus RNA-dependent RNA polymerase inhibitors: structure-based screens and molecular dynamics for the pursue of new poly pharmacological inhibitors. *BMC Bioinformatics* **2012**, *13* (Suppl 17), S5.
- (15) Kumar, A.; Siddiqi, M. I. Virtual screening against *Mycobacterium tuberculosis* dihydrofolate reductase: suggested workflow for compound prioritization using structure interaction fingerprints. *J. Mol. Graph. Model.* **2008**, *27* (4), 476–488.
- (16) Kumar, A.; Chaturvedi, V.; Bhatnagar, S.; Sinha, S.; Siddiqi, M. I. Knowledge based identification of potent antitubercular compounds using structure based virtual screening and structure interaction fingerprints. *J. Chem. Inf. Model.* **2009**, *49* (1), 35–42.
- (17) Kumar, V.; Khan, S.; Gupta, P.; Rastogi, N.; Mishra, D. P.; Ahmed, S.; Siddiqi, M. I. Identification of novel inhibitors of human Chk1 using pharmacophore-based virtual screening and their evaluation as potential anti-cancer agents. *J. Comput. Aided Mol. Des.* **2014**, *28* (12), 1247–1256.
- (18) Hou, Z.; Nakanishi, I.; Kinoshita, T.; Takei, Y.; Yasue, M.; Misu, R.; Suzuki, Y.; Nakamura, S.; Kure, T.; Ohno, H.; Murata, K.; Kitauro, K.; Hirasawa, A.; Tsujimoto, G.; Oishi, S.; Fujii, N. Structure-based design of novel potent protein kinase CK2 (CK2) inhibitors with phenyl-azole scaffolds. *J. Med. Chem.* **2012**, *55* (6), 2899–2903.
- (19) Shah, P.; Tiwari, S.; Siddiqi, M. I. Integrating molecular docking, CoMFA analysis and Machine Learning classification with virtual screening towards identification of novel scaffolds as *Plasmodium falciparum* enoyl acyl carrier protein reductase inhibitor. *Medicinal Chemistry Research* **2014**, *23* (7), 3308–3326.
- (20) Scherr, N.; Honnappa, S.; Kunz, G.; Mueller, P.; Jayachandran, R.; Winkler, F.; Pieters, J.; Steinmetz, M. O. Structural basis for the specific inhibition of protein kinase G, avirulence factor of *Mycobacterium tuberculosis*. *Proc. Natl. Acad. Sci. U. S. A.* **2007**, *104* (29), 12151–12156.
- (21) Anand, N.; Singh, P.; Sharma, A.; Tiwari, S.; Singh, V.; Singh, D. K.; Srivastava, K. K.; Singh, B. N.; Tripathi, R. P. Synthesis and evaluation of small libraries of triazolylmethoxy chalcones, flavanones and 2-aminopyrimidines as inhibitors of mycobacterial FAS-II and PknG. *Bioorg. Med. Chem.* **2012**, *20* (17), 5150–5163.
- (22) SYBYL-X, version 2.0; Tripos, Certara, 1991–2012.
- (23) Jones, G.; Willett, P.; Glen, R. C. A genetic algorithm for flexible molecular overlay and pharmacophore elucidation. *J. Comput. Aided Mol. Des.* **1995**, *9* (6), 532–549.
- (24) Olah, M.; Mracec, M.; Ostopovici, L.; Rad, R.; Bora, A.; Hadaruga, N.; Olah, I.; Banda, M.; Simon, Z.; Oprea, T. I. WOMBAT: World of molecular bioactivity. *Chemoinf. Drug Discovery* **2004**, *1*, 223–239.
- (25) <http://www.maybridge.com/> (march 7, 2013).
- (26) Jain, A. N. Surflex: fully automatic flexible molecular docking using a molecular similarity-based search engine. *J. Med. Chem.* **2003**, *46* (4), 499–511.
- (27) Rarey, M.; Kramer, B.; Lengauer, T.; Klebe, G. A fast flexible docking method using an incremental construction algorithm. *J. Mol. Biol.* **1996**, *261* (3), 470–489.
- (28) Morris, G. M.; Huey, R.; Lindstrom, W.; Sanner, M. F.; Belew, R. K.; Goodsell, D. S.; Olson, A. J. AutoDock4 and AutoDockTools4: Automated docking with selective receptor flexibility. *J. Comput. Chem.* **2009**, *30* (16), 2785–2791.
- (29) Leonard, B.; Coronel, J.; Siedner, M.; Grandjean, L.; Caviedes, L.; Navarro, P.; et al. Inter- and intra-assay reproducibility of microplate Alamar blue assay results for isoniazid, rifampicin, ethambutol, streptomycin, ciprofloxacin, and capreomycin drug susceptibility testing of *Mycobacterium tuberculosis*. *Journal of clinical microbiology* **2008**, *46*, 3526–3529.
- (30) O'Brien, J.; Wilson, I.; Orton, T.; Pognan, F. Investigation of the Alamar Blue (resazurin) fluorescent dye for the assessment of mammalian cell cytotoxicity. *European journal of biochemistry/FEBS* **2000**, *267*, 5421–5426.
- (31) Hess, B.; Kutzner, C.; van der Spoel, D.; Lindahl, E. GROMACS 4: Algorithms for Highly Efficient, Load-Balanced, and Scalable Molecular Simulation. *J. Chem. Theory Comput.* **2008**, *4* (3), 435–447.
- (32) Smale, S. T. Luciferase assay. *Cold Spring Harbor Protocols* **2010**, DOI: 10.1101/pdb.prot5421.